Hindawi Publishing Corporation
Advances in Condensed Matter Physics
Volume 2014, Article ID 806327, 6 pages
http://dx.doi.org/10.1155/2014/806327

Research Article

Defects Induced Room Temperature Ferromagnetism in ZnO Thin Films

Xiao Zhang, Wei Zhang, Xinghua Zhang, Xuewen Xu, Fanbin Meng, and C. C. Tang

School of Materials Science and Engineering, Hebei University of Technology, Tianjin 300130, China

Correspondence should be addressed to Xiao Zhang; zhangxiaonk@gmail.com and C. C. Tang; tangcc@hebut.edu.cn

Received 2 December 2013; Accepted 27 December 2013; Published 19 February 2014

Academic Editor: Shoubao Zhang

Polycrystalline ZnO thin films are prepared by the co-sputtering method under different oxygen partial pressures. Films deposited in pure argon gas exhibit ferromagnetism, whereas other films deposited under different oxygen partial pressures are diamagnetism. XPS results show the presence of Zn interstitial and oxygen vacancy in all of samples. Further analysis indicates that Zn interstitial may play an important role in triggering magnetic order on the undoped ZnO thin films by inducing an alteration of electronic configuration.

1. Introduction

ZnO-based dilute magnetic semiconductors (DMSs) have attracted intense interests due to their potential applications in spintronic devices [1]. Room temperature (RT) ferromagnetism (FM) has been reported theoretically and experimentally in magnetic transition metal doped ZnO nanoparticles and thin films [2–7]. However, several works pointed out that the transition metal dopants are not essential in the observed ferromagnetism. For instance, the results of X-ray magnetic circular dichroism spectra showed that the magnetism in Mn doped ZnO nanoparticle and thin films is critically sensitive to defects other than the transition metal dopants themselves [8] and bulk ZnO doped with Co, Mn, or Cr shows paramagnetism [6, 9, 10]. Meanwhile, RT FM was observed in nonmagnetic ion doped ZnO thin films and nanoparticles [11–13] and even undoped ZnO films [14–17], nanoparticles [18, 19], or partially oxidized Zn nanowires [20, 21], which indicates that the RT FM observed in ZnO matrix may be intrinsic. It is restricted to some defect-rich regions, such as the surface, interface, and grain boundary, not uniform throughout the samples [22]. On the other hand, the indirect exchange interaction models such as Zener/Ruderman-Kittel-Kasuya-Yosida (RKKY)-type exchange, double- and super-exchange, F-center-mediated bound magnetic polaron models, are hard to explain the observed RT FM induced by only few percent of magnetic ions. Thus, the intrinsic defects should be important on the FM order in ZnO-based DMSs. However, which kinds of defects play an important role, how the defects facilitate the magnetic coupling, and how to control these defects are still under intensive debate. Some reports demonstrated that RT FM could stem from the lattice defects such as oxygen vacancy (V_O) or Zn interstitial (Zn_i) in pure ZnO thin films, nanoparticles, and nanowires [17, 23–26]. Straumal et al. [27] demonstrated that FM only appears if the ratio of grain-boundary area to grain volume exceeds a certain threshold value. Sanchez et al. [28] predicted that varying the hydrogen density on the ZnO (0001) surface can achieve reversible switch of surface FM. More interestingly, even absorbing certain organic molecules can induce ferromagnetic-like behavior in undoped ZnO nanoparticles [29]. These results challenge the understanding of the origin and mechanism of FM.

So far, although lots of works have been carried out to explore the origin of RT FM in undoped ZnO, the results are far from convincing and even some of the results are inconsistent, partly because ZnO is a semiconducting material with many species of native defects with quite a few of them behaving as shallow donors. Now, it is known that the native defects depend strongly on preparation methods and conditions. ZnO materials prepared by various methods from different

groups generally show significant differences in physical properties including native defect/impurity species and density, mobility, and crystallinity. When these ZnO materials are employed for DMSs study, it is not a surprise that distinct results were reported even with similar conditions. Therefore, it is the most important to elucidate the effect of specific film-growth conditions. In this study, polycrystalline ZnO films were fabricated under different oxygen partial pressure (P_{O_2}). The experimental results show that the only RT FM observed in ZnO film deposited under pure Ar and saturated magnetization is 0.89 emu/cc, while other samples deposited under Ar and O_2 mixture are diamagnetism. After depositing a single Zn layer on the magnetic film and annealing the sample at high temperature, the saturated magnetization significantly increased to 1.62 emu/cc. These results suggest that the Zn interstitial may be a response to the origin of FM order in pure ZnO thin films.

2. Experiments

A series of polycrystalline ZnO films were fabricated by RF-sputtering ZnO (99.99%) targets in Ar (99.999%) and O_2 (99.999%) mixture at room temperature. The base pressure of the chamber was better than 1×10^{-5} Pa before deposition and the total pressure for sputtering was kept at 2.0 Pa. The RF-sputtering power of ZnO target was kept at 260 W. The films were deposited on glass and kapton substrates for the measurements of structural and transport properties, respectively. To eliminate the spurious magnetic data, the samples and polymer tweezers were cleaned with acetone prior to measurement. The films thickness was kept at 200 nm. The microstructure of the films was characterized by X-ray diffraction pattern (XRD) with Cu K_α radiation ($\lambda = 0.15418$) using X' Pert PRO machine. The composition and chemical states of ZnO thin films were examined by X-ray photoelectron spectroscopy (XPS) and auger electron spectroscopy (AES) using Physical Electronic Spectrometry machine. The DC electrical resistivity measurements were measured using a conventional four-probe method performed in a Quantum Design PPMS. The magnetization measurements were carried out using a Quantum Design vibrating sample magnetometry.

3. Results and Discussion

Figure 1(a) shows the XRD pattern of the ZnO polycrystalline samples fabricated under different oxygen partial pressure (P_{O_2}). The results indicate that all samples have highly (00l)-preferred orientation in contrast to the standard diffraction pattern of wurtzite ZnO. The particle size can be derived from the Scherrer formula [30]:

$$D_{hkl} = \frac{0.9\lambda}{\beta \cos\theta}, \quad (1)$$

where D_{hkl} is the particle size along (hkl) direction, β is the full width at half maximum (FWHM) of the XRD peak, $\lambda = 0.154058$ nm is the wavelength of Cu K_α radiation, and θ is the Bragg angle. Figure 1(b) shows the relation between obtained particle size using the FWHM of (002) peaks and P_{O_2}. It can be seen that there is not monotonic dependence of particle size on the P_{O_2}. At low P_{O_2}, the particle size increases with increasing P_{O_2}, reaches the maximum value at $P_{O_2} = 1$ Pa, and then decreases to 42.7(9) at $P_{O_2} = 1.5$ Pa. With the P_{O_2} increasing, the particle size of the ZnO thin films tends to be a constant.

The composition and chemical states of the ZnO thin films deposited under $P_{O_2} = 0$ Pa and $P_{O_2} = 2$ Pa are further investigated by XPS analysis. Samples were etched by Ar^+ bombardment (5×10^5 Torr) for 5 min to examine the intrinsic chemical state of each element in the films. A broad scan survey spectrum indicates that only Zn, O, and C elements exist and no other detectable contaminated element above 0.1% exists in the ZnO samples. As shown in Figure 2(a) the peak positions of Zn $2p_{1/2}$ and Zn $2p_{3/2}$ are similar in both samples. Comparing the XPS standard spectra of Zn $2p$ [30], it is concluded that the valence state of Zn element is +2. On the other hand, the peaks of Zn $2p_{3/2}$ in both samples exhibit slight asymmetry. Islam group has analyzed the Zn $2p_{3/2}$ peak of ZnO thin film systematically and attributed this kind of asymmetry of Zn $2p_{3/2}$ peak to the existence of excess zinc in the films [31]. No such asymmetry is observed for hydrogen-annealed pure ZnO films. But the exact nature of the distribution of Zn in the ZnO matrix remains under investigation. In order to confirm the existence of zinc in the films, AES measurements were carried out. Figure 2(b) presents a Zn($L_3M_{45}M_{45}$) AES signal of the ZnO samples deposited under $P_{O_2} = 0$ Pa and $P_{O_2} = 2$ Pa. The major peaks at 264.2 eV are considered to be associated with Zn^{2+} in ZnO matrix. The minor one at 261.2 eV is due to Zn of metallic Zn or Zn_i in ZnO matrix lattice. It can be seen that the peak intensity at 261.2 eV for the sample deposited under $P_{O_2} = 0$ Pa is significantly larger than that for sample prepared under $P_{O_2} = 2$ Pa. It implies that more metallic Zn or Zn_i can be generated under oxygen-deficient atmosphere.

Deeper insight into the chemical states of oxygen is achieved through the analysis of the O 1*s* peaks of ZnO polycrystalline samples deposited under $P_{O_2} = 0$ Pa and $P_{O_2} = 2$ Pa, as shown in Figure 3. The broad and asymmetric O 1*s* peaks could be consistently fitted by a Gaussian function to separate the multicomponent oxygen species, which centered at 530.0±0.1 eV, 531.5±0.1 eV, and 532.3±0.1 eV, respectively. The component on the low binding energy side of the O 1*s* at 530.0 ± 0.1 eV is attributed to O^{2-} ions in wurtzite structure of hexagonal Zn^{2+} ion array, surrounded by Zn atoms with their full complement of the nearest neighboring O^{2-} ions [32]. In other words, the intensity of this component is the indicator of the amount of oxygen atoms in a fully oxidized, stoichiometric surrounding. The medium binding energy component at 531.5 ± 0.1 eV may partially be associated with O^{2-} ions that are in oxygen-deficient regions within the matrix. Thus, the variation of the relative intensity ratio of medium component to total O 1*s* may be connected in part to the variations in the concentration of oxygen vacancies. It can be seen that this ratio for the sample prepared without O_2 is remarkably larger than the sample deposited under $P_{O_2} = 2$ Pa. It is consistent with AES results of Zn; that is,

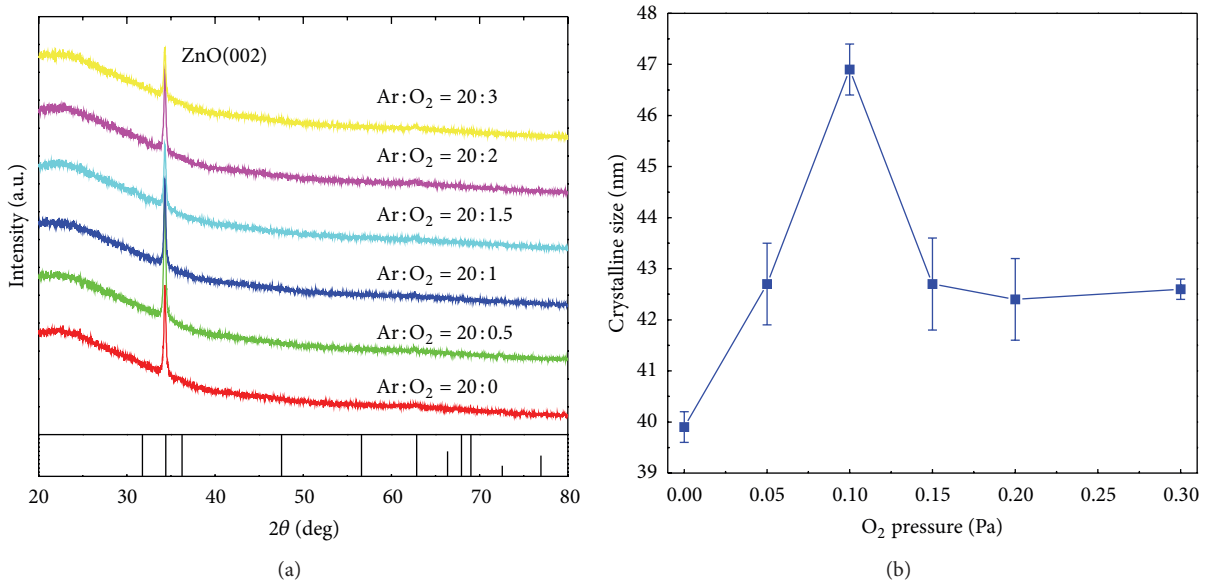

FIGURE 1: (a) XRD patterns of ZnO polycrystalline thin films deposited under different oxygen partial pressure; (b) the average grains diameters as a function of oxygen partial pressure estimated by the Scherrer equation.

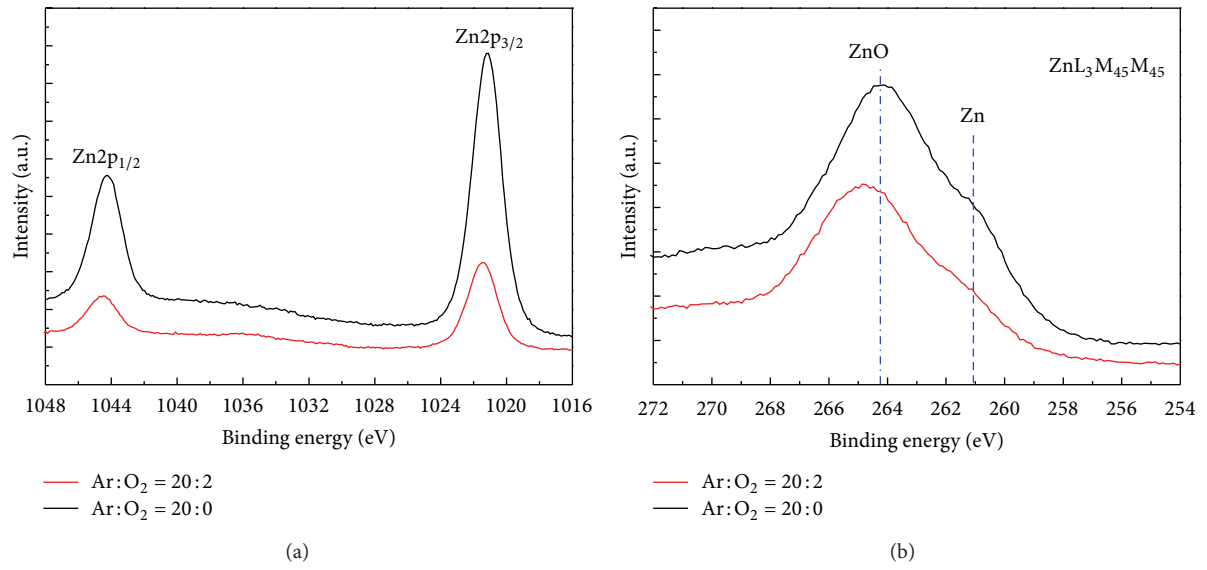

FIGURE 2: (a) XPS data of Zn 2p and (b) AES data of Zn LMM in ZnO films deposited under $P_{O_2} = 0$ Pa and $P_{O_2} = 2$ Pa.

without O_2, more Zn_i and V_O appear when compared to the sample deposited under O_2. Finally, the appearance of the high binding energy component at 532.3±0.1 eV indicates the presence of loosely bound oxygen in the ZnO films belonging to specific species, such as adsorbed H_2O or adsorbed O_2, which is difficult to remove by just increasing P_{O_2} during deposition process.

Figure 4 shows magnetization loops of ZnO films deposited under different P_{O_2}. The applied magnetic field was parallel to the surface of the sample. The data in the main figure is M-H curves before the subtraction of the diamagnetic signal of samples, which indicates the sample prepared under $P_{O_2} = 0$ Pa shows RT FM. Upper inset of Figure 3 obtained from subtracting the saturated linear parts of the measured signal shows typical hysteresis behaviors and the saturated magnetization is 0.89 emu/cc. However, other samples deposited under different oxygen partial pressure are diamagnetic, confirming that no FM impurities were introduced during the preparation of the films. It should be noted that FM behavior and average grains diameters upon different oxygen partial pressure have different trends. It implies that the average grains sizes are indirectly related

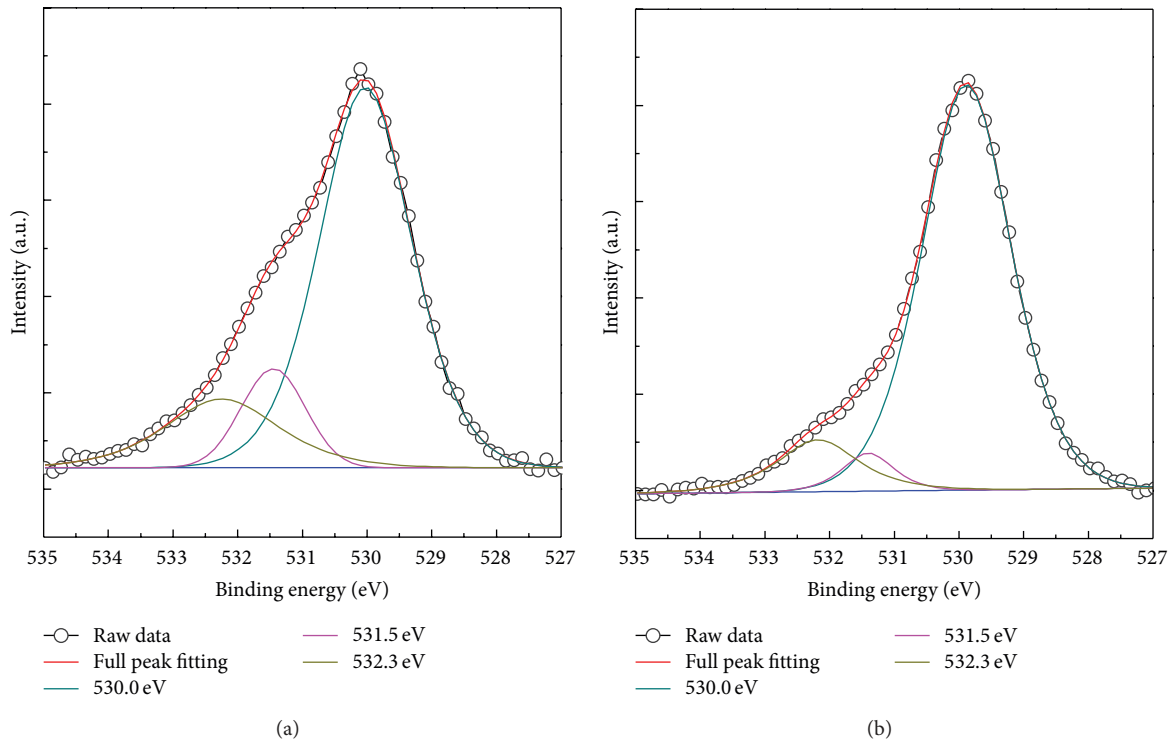

FIGURE 3: XPS data of O 1*s* and its Gaussian-resolved component for the sample deposited under (a) $P_{O_2} = 0$ Pa and (b) $P_{O_2} = 2$ Pa, respectively.

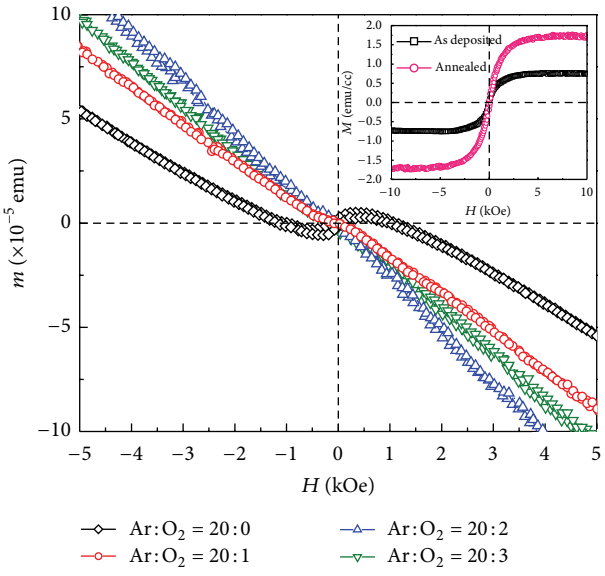

FIGURE 4: *M*-*H* curves for ZnO thin films deposited under different oxygen partial pressure at 300 K. Upper inset: *M*-*H* curves of ZnO as-deposited and annealed films deposited under $P_{O_2} = 0$ Pa at 300 K after the subtraction of the diamagnetic signal.

to the FM in undoped ZnO films. On the other hand, the measured resistivity of the samples deposited under $P_{O_2} = 0$ Pa is $6.5(2) \times 10^4\ \Omega$ cm at RT.

Indeed, the origin of RT FM in undoped ZnO is still a controversial issue. Many hypotheses have been presented to give a reasonable interpretation for the origin of the RT FM in pure ZnO. Since the sample deposited under $P_{O_2} = 0$ Pa is insulators, the carrier-mediated RKKY-type model seems not to be applicable. According to previous work [23–26], the origin of the room temperature FM of undoped ZnO is due to the introduction of Zn_i and/or V_O defects rather than Zn vacancies (V_{Zn}), because formation energy of V_{Zn} is so high that it could not preferably form in ZnO. The chemical states of Zn and O ions in ZnO samples deposited under different P_{O_2} show that Zn_i and V_O coexist in the as-deposited samples. As P_{O_2} increases, both of the Zn_i and V_O are decreasing meanwhile the FM disappears at higher P_{O_2}. Thus, the Zn_i and/or V_O should contribute to the origin of FM in pure ZnO thin films. To further confirm which kind of defect plays a more important role in the origin of FM in the sample, a layer of pure Zn with thickness of about 70 nm was deposited on the ZnO film deposited under $P_{O_2} = 0$ Pa. Then, the sample was heated in high vacuum at 300°C for 10 min. Because the diffusion of Zn is easier than that of oxygen [33] and there are not enough oxygen atoms from the air which can diffuse in the lattice to oxidize the diffused Zn, Zn_i will generate and be trapped in the lattice, which leads to the increase in defect density of Zn_i. On the other hand, magnetic measurement indicates that the saturated magnetization of annealed sample increases to 1.62 emu/cc. Thus, Zn_i not V_O should be responsible for the observed weak RT FM in as-deposited sample and the significant increase of M_s in the annealed sample.

Theoretical calculation indicated that the level of Zn_i lies close to the bottom of the conduction band (shallow donors), which will induce strong interaction between the localized interstitial Zn 4*s* level and the conduction band [5]. This interaction alternates the electronic structure, leading to ferromagnetic-like behavior. It should be noted that this modification of the semiconductor electronic structure can be realized in the absence of the magnetic ions. More generally, other methods inducing such kind of shallow donors will also alternate the electronic structure and result in the RT FM, such as fabricating ZnO low dimensional nanoparticles with more intrinsic defects, capping with organic molecules into ZnO nanoparticle [29] and producing more defects by mechanical milling in ZnO nanoparticles [23].

4. Conclusions

In summary, RT FM is observed in undoped ZnO thin films deposited without oxygen, while other samples deposited under different P_{O_2} are all diamagnetism. After depositing a single Zn layer on the magnetic ZnO thin films and annealing the sample at high temperature, the saturated magnetization significantly increased. All results indicate that the origin of FM order in pure ZnO films should be related to the Zn_i defects. The shallow donor caused by Zn_i defects might modify the electronic structure of undoped ZnO thin films, leading to the RT FM. Our result will help to get further insight into the ferromagnetic origin in undoped ZnO systems.

Conflict of Interests

The authors declare that there is no conflict of interests regarding the publication of this paper.

Acknowledgments

This work was supported by the National Natural Science Foundation of China (Grant nos. 51102075, 51171056, and 51371075) and the Key Project of Science and Technology for Colleges in Hebei Province, China (Grant no. ZD2010120).

References

[1] S. A. Wolf, D. D. Awschalom, R. A. Buhrman et al., "Spintronics: a spin-based electronics vision for the future," *Science*, vol. 294, no. 5546, pp. 1488–1495, 2001.

[2] T. Dietl, H. Ohno, F. Matsukura, J. Cibert, and D. Ferrand, "Zener model description of ferromagnetism in zinc-blende magnetic semiconductors," *Science*, vol. 287, no. 5455, pp. 1019–1022, 2000.

[3] J. M. D. Coey, M. Venkatesan, and C. B. Fitzgerald, "Donor impurity band exchange in dilute ferromagnetic oxides," *Nature Materials*, vol. 4, no. 2, pp. 173–179, 2005.

[4] H. Gu, W. Zhang, Y. Xu, and M. Yan, "Effect of oxygen deficiency on room temperature ferromagnetism in Co doped ZnO," *Applied Physics Letters*, vol. 100, no. 11, Article ID 202401, 2012.

[5] C. H. Patterson, "Role of defects in ferromagnetism in Zn1−xCoxO: a hybrid density-functional study," *Physical Review B*, vol. 74, no. 14, Article ID 144432, 2006.

[6] H. Liu, X. Zhang, L. Li et al., "Role of point defects in room-temperature ferromagnetism of Cr-doped ZnO," *Applied Physics Letters*, vol. 91, no. 7, Article ID 072511, 2007.

[7] J. M. Baik, T. W. Kang, and J.-L. Lee, "Effects of N_2O plasma treatment on magnetic properties of (Zn, Mn)O nanorods," *Nanotechnology*, vol. 18, no. 9, Article ID 095703, 2007.

[8] K. R. Kittilstved, W. K. Liu, and D. R. Gamelin, "Electronic structure origins of polarity-dependent high-T_c ferromagnetism in oxide-diluted magnetic semiconductors," *Nature Materials*, vol. 5, no. 4, pp. 291–297, 2006.

[9] J. Alaria, P. Turek, M. Bernard et al., "No ferromagnetism in Mn doped ZnO semiconductors," *Chemical Physics Letters*, vol. 415, no. 4–6, pp. 337–341, 2005.

[10] S. Yin, M. X. Xu, L. Yang et al., "Absence of ferromagnetism in bulk polycrystalline $Zn_{0.9}Co_{0.1}O$," *Physical Review B*, vol. 73, no. 22, Article ID 224408, 2006.

[11] M. Venkatesan, C. B. Fitzgerald, J. G. Lunney, and J. M. D. Coey, "Anisotropic ferromagnetism in substituted zinc oxide," *Physical Review Letters*, vol. 93, no. 17, Article ID 177206, p. 1, 2004.

[12] H. Pan, J. B. Yi, L. Shen et al., "Room-temperature ferromagnetism in carbon-doped ZnO," *Physical Review Letters*, vol. 99, no. 12, Article ID 127201, 2007.

[13] C.-F. Yu, T.-J. Lin, S.-J. Sun, and H. Chou, "Origin of ferromagnetism in nitrogen embedded ZnO:N thin films," *Journal of Physics D*, vol. 40, no. 21, pp. 6497–6500, 2007.

[14] Q. Xu, H. Schmidt, S. Zhou et al., "Room temperature ferromagnetism in ZnO films due to defects," *Applied Physics Letters*, vol. 92, no. 8, Article ID 082508, 2008.

[15] S. Ghoshal and P. S. Anil Kumar, "Suppression of the magnetic moment upon Co doping in ZnO thin film with an intrinsic magnetic moment," *Journal of Physics Condensed Matter*, vol. 20, no. 19, Article ID 192201, 2008.

[16] M. Kapilashrami, J. Xu, V. Ström, K. V. Rao, and L. Belova, "Transition from ferromagnetism to diamagnetism in undoped ZnO thin films," *Applied Physics Letters*, vol. 95, no. 3, Article ID 033104, 2009.

[17] N. H. Hong, J. Sakai, and V. Brizé, "Observation of ferromagnetism at room temperature in ZnO thin films," *Journal of Physics Condensed Matter*, vol. 19, no. 3, Article ID 036219, 2007.

[18] Z. Yan, Y. Ma, D. Wang et al., "Impact of annealing on morphology and ferromagnetism of ZnO nanorods," *Applied Physics Letters*, vol. 92, no. 8, Article ID 081911, 2008.

[19] J. B. Yi, H. Pan, J. Y. Lin et al., "Ferromagnetism in ZnO nanowires derived from electro-deposition on AAO template and subsequent oxidation," *Advanced Materials*, vol. 20, no. 6, pp. 1170–1174, 2008.

[20] L. Y. Li, Y. H. Cheng, X. G. Luo et al., "Room-temperature ferromagnetism and the scaling relation between magnetization and average granule size in nanocrystalline Zn/ZnO core-shell structures prepared by sputtering," *Nanotechnology*, vol. 21, no. 14, Article ID 145705, 2010.

[21] Z. Yang, "A perspective of recent progress in ZnO diluted magnetic semiconductors," *Applied Physics A*, vol. 112, no. 2, pp. 241–254, 2013.

[22] J. M. D. Coey, K. Wongsaprom, J. Alaria, and M. Venkatesan, "Charge-transfer ferromagnetism in oxide nanoparticles," *Journal of Physics D*, vol. 41, no. 13, Article ID 134012, 2008.

[23] T. L. Phan, Y. D. Zhang, D. S. Yang, N. X. Nghia, T. D. Thanh, and S. C. Yu, "Defect-induced ferromagnetism in ZnO nanoparticles prepared by mechanical milling," *Applied Physics Letters*, vol. 102, no. 7, Article ID 072408, 2013.

[24] S. Banerjee, M. Mandal, N. Gayathri, and M. Sardar, "Enhancement of ferromagnetism upon thermal annealing in pure ZnO," *Applied Physics Letters*, vol. 91, no. 18, Article ID 182501, 2007.

[25] M. H. F. Sluiter, Y. Kawazoe, P. Sharma et al., "First principles based design and experimental evidence for a ZnO-based ferromagnet at room temperature," *Physical Review Letters*, vol. 94, no. 18, Article ID 187204, 2005.

[26] X. Zhang, Y. H. Cheng, L. Y. Li et al., "Evidence for high-T_c ferromagnetism in Zn_x $(ZnO)_{1-x}$ granular films mediated by native point defects," *Physical Review B*, vol. 80, no. 17, Article ID 174427, 2009.

[27] B. B. Straumal, A. A. Mazilkin, S. G. Protasova et al., "Magnetization study of nanograined pure and Mn-doped ZnO films: formation of a ferromagnetic grain-boundary foam," *Physical Review B*, vol. 79, no. 20, Article ID 205206, 2009.

[28] N. Sanchez, S. Gallego, J. Cerdá, and M. C. Muñoz, "Tuning surface metallicity and ferromagnetism by hydrogen adsorption at the polar ZnO(0001) surface," *Physical Review B*, vol. 81, no. 11, Article ID 115301, 2010.

[29] M. A. Garcia, J. M. Merino, E. F. Pinel et al., "Magnetic properties of ZnO nanoparticles," *Nano Letters*, vol. 7, no. 6, pp. 1489–1494, 2007.

[30] B. D. Cullity, *Elements of X-Ray Diffraction*, Addison-Wesley Publication, New York, NY, USA, 1978.

[31] M. N. Islam, T. B. Ghosh, K. L. Chopra, and H. N. Acharya, "XPS and X-ray diffraction studies of aluminum-doped zinc oxide transparent conducting films," *Thin Solid Films*, vol. 280, no. 1-2, pp. 20–25, 1996.

[32] J. C. C. Fan and J. B. Goodenough, "X-ray photoemission spectroscopy studies of Sn-doped indium-oxide films," *Journal of Applied Physics*, vol. 48, no. 8, pp. 3524–3531, 1977.

[33] K. R. Kittilstved, D. A. Schwartz, A. C. Tuan, S. M. Heald, S. A. Chambers, and D. R. Gamelin, "Direct kinetic correlation of carriers and ferromagnetism in Co^{2+}:ZnO," *Physical Review Letters*, vol. 97, no. 3, Article ID 037203, 2006.